## SUPPLEMENTAL DATA

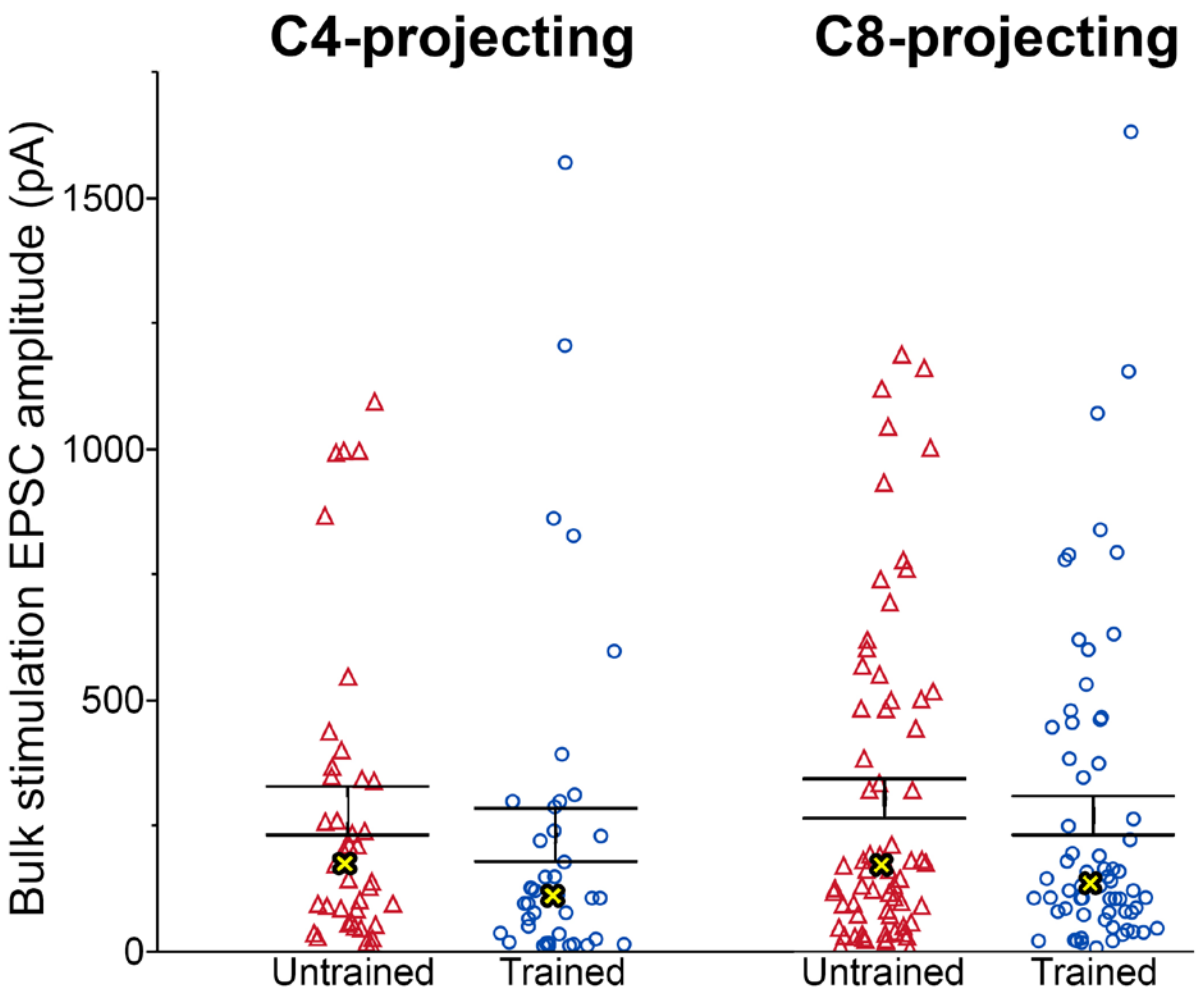


**Figure S1 [related to Figure 2]. Non-normalized bulk stimulation EPSC peak amplitude.**

Average EPSC peak amplitude for individual corticospinal cells in response to bulk stimulation of thalamocortical axons expressing ChR2. Data are not normalized for variable expression across slices/animals. Thus, the quantity of presynaptic terminals activated varied across recorded cells, producing large variability in EPSC amplitude. For normalized data, see Figure 2. The data presented here include recordings of cell pairs (which are included in Figure 2), as well as individually recorded cells (not included in Figure 2). Error bars = SEM, centered over the mean. Yellow X = median.

## SUPPLEMENTAL EXPERIMENTAL PROCEDURES

A total of 86 male F344 rats were subjects of this study, 55 of which were included for paired recording experiments (bulk stimulation, MK-801, and/or AMPA:NMDA experiments), 19 for strontium experiments, and 12 for minimal optical stimulation experiments. All procedures and animal care adhered to American Association for the Accreditation of Laboratory Animal Care and institutional guidelines. Animals were group housed (2-3 per cage) on a 12 h light/dark cycle. Each cage was enriched with a cardboard tube. Cage tops were comprised of metal bars, which animals climb and hang from.

Labeling of corticospinal subpopulations: To label corticospinal neurons projecting to the C8 cervical spinal cord, animals of approximate postnatal age 35 days were anesthetized with a cocktail (2 ml/kg) containing ketamine (25 mg/mL), xylazine (1.3 mg/mL), and acepromazine (0.25 mg/mL). The overlying dura between C7 and T1 was resected and a glass micropipette (tip < 40 µm) containing red or green fluorescent latex microspheres (Lumafluor, Durham, NC) was inserted into the dorsal horn of the spinal cord. Using a Picospritzer II (General Valve), ~350 nL of fluorescent latex microspheres was injected into each side of the spinal cord. To label corticospinal neurons projecting to the upper cervical spinal cord (C4), the same procedure was repeated between C3 and C4 spinal vertebra, using a different colored dye (green or red) than that used for C8 injections. In all cases, tracer diffusion was assessed postmortem in 50 µm coronal slices of the spinal cord. Animals with tracer diffusion into the dorsal columns were excluded from further study. A minority of cells (~25%) expressed colocalization of unique tracers injected into C4 and C8 (see (Biane et al., 2015)); such double-labeled neurons were excluded from the current study.

Viral injections: AAV2/2-CaMKIIa-hChR2 (E123T/T159C (Berndt et al., 2011), produced by UNC vector core) was targeted to the VA/VL via bilateral injections at two sites per hemisphere (injection site 1: -2.3 A/P, 1.6 M/L, -5.7 D/V; injection site 2: -2.6 A/P, 1.7 M/L, -5.8 D/V; A/P and M/L relative to bregma, D/V relative to pia). An infusion pump delivered 0.2 µl at each site at a rate of 0.12 µl/min. Following infusion, the pipette (tip < 40 µm) remained in place for four minutes to allow adequate diffusion to the surrounding tissue. Infected animals typically displayed robust axon expression of ChR2 within M1. Cell bodies positive for ChR2 were not detected in any cortical layer, indicating the virus did not retrogradely infect corticothalamic neurons and that the virus did not leak appreciably along the pipette tract.

Skilled forelimb grasp training: Skilled motor training was performed using a single-pellet reaching task as previously described (Conner et al., 2003; Whishaw, 2000). Animals were randomly assigned to experimental groups. “Trained” rats were shaped to reach through a small window to retrieve a single sugar pellet (Test Diets) from a well located 2 cm beyond the testing chamber. Food restriction to ~90% free-feeding baseline was utilized

to increase motivation. Daily training consisted of placing the rat into the test box until the rat had made 60 reaches (usually < 7 min). A "reach" was scored when the rat extended its forelimb through the slot. A "hit" was scored if the rat successfully brought the pellet back to his mouth for consumption. Across all experiments, a combined N = 46 animals were trained. Training data are collapsed across all experiments. All training was conducted during the light cycle at consistent times.

Untrained control rats were similarly food restricted, and spent equivalent time in the testing chamber, but were not permitted to reach for reward pellets. Untrained animals received a similar number of reward pellets as their trained counterparts, with small forceps used to deliver single pellets directly into the animal's mouth.

Electrophysiological slice preparation: One to five days following termination of skilled forelimb grasp training, young adult rats (P55 – 59) were anesthetized and perfused for 3 minutes with ice-cold, oxygenated, modified sucrose artificial cerebrospinal fluid (ACSF) containing (in mM) 75 NaCl, 2.5 KCl, 3.3 $MgSO_4$, 0.5 $CaCl_2$, $1NaH_2PO_4$, 26.2 $NaHCO_3$, 22 glucose, 52.6 sucrose, 10 HEPES, 10 choline chloride, 1 pyruvate, 1 L-ascorbic acid (~300 mOsml, pH 7.4). The brain was rapidly dissected and 330 μm-thick slices spanning the motor cortex were cut at 15° anterior to the mid-coronal plane to match the dendritic projection pattern of layer 5 corticospinal neurons (Wang et al., 2011). Slices were transferred to an opaque interface chamber containing the same modified sucrose ACSF solution and incubated at 34° C for 30 min. Slices were then held at room temperature (23° C) in the interface chamber for at least 45 min before initiating recordings. Recordings were made in a submersion-type recording chamber and, unless otherwise noted, perfused with oxygenated ACSF containing (in mM) 119 NaCl, 2.5 KCl, 2 $MgCl_2$, 2.5 $CaCl_2$, 1.3 $NaH_2PO_4$, 26.0 $NaHCO_3$, 20 glucose (~295 mOsml) at 23° C at a rate of 2-3 ml / minute.

Electrophysiology and photostimulation: Whole-cell patch clamp recordings were obtained using Multiclamp 700B patch amplifiers (Molecular Devices) and data analyzed using pClamp 10 software (Molecular Devices). Data were low-pass filtered at 2 kHz, and digitized at 10 kHz. Data were collected from cells greater than 25 μm below the cutting plane of the slice surface (mean cell depth from slice surface ± SD = 64 ± 22 μm). During recordings, the experimenter was blinded to the experimental group and retrograde tracer assignment of tissue.

All recordings were performed within the caudal forelimb area of the primary motor cortex. Neurons near the center of the ChR2-expressing axon band in L5 were targeted for recording, and were selected based on retrograde bead emission spectra (red or green), reflecting tracers injected at either the C8 or C4 spinal segment; individual cells expressing both red and green retrograde tracers were not targeted. Cells were then visualized under infrared differential interference contrast videomicroscopy (Olympus BX-51W scope and Rolera XR digital

camera) for whole-cell patch clamp. Due to variable ChR2 expression across animals and slices, an internal slice control was used to normalize responses. Thus, neighboring C4- and C8-projecting neurons were targeted for simultaneous whole-cell patch clamp in up to four retrogradely labeled cells (mean intersomatic distance between recorded cell pairs ± SD = 92 ± 53 μm). In cases where an internal control was unnecessary (strontium, minimal optical stimulation, AMPA:NMDA, and MK-801 experiments), data were typically collected in the absence of paired recordings.

Whole-cell voltage and current clamp recordings were made at room temperature using pulled patch pipettes (5-6 MΩ) filled with internal solution containing (in mM) 150 K-Gluconate, 1.5 $MgCl_2$, 5.0 HEPES, 1 EGTA, 10 phosphocreatine, 2.0 ATP, and 0.3 GTP, unless otherwise noted. Data were analyzed exclusively from cells with a resting membrane potential ≤ -50 mV, with drift less than 6 mV over the entire recording period, with access resistance ≤ 35 MΩ, with the ability to evoke multiple spikes with >60 mV peak amplitude from threshold, and located greater than 25 μm below the cutting plane of the slice surface. Series resistance compensation (70%) was applied during minimal optical stimulation and strontium-evoked asynchronous release recordings. For all other experiments, series resistance was not compensated, but was continuously monitored via negative voltage steps.

Blue light was delivered through a 5x objective (range of intensity at tissue: 2 – 4 $mW/mm^2$), creating an area of light stimulation that spanned 1000s of μm and ensuring uniform activation of ChR2-expressing axon terminals across simultaneously patched neighboring cells. Light emission originated from an arc lamp passing through a FITC excitation filter (Chroma) and controlled by a SmartShutter (Sutter Instruments) with a 1ms open time, unless otherwise noted (e.g., minimal optical stimulation and strontium experiments).

ChR2-mediated thalamocortical signaling: Postsynaptic responses due to bulk photo-stimulation of thalamocortical axons were evaluated over 10-30 sweeps. Paired light pulses were delivered 50 ms apart, and postsynaptic responses were monitored in cells held at -65 mV in voltage clamp. Individual sweeps were separated by 25 s. Occasionally, polysynaptic activity was observed across cell pairs, as demonstrated by multiple peaks in the EPSC trace. When a monosynaptic response could not be clearly identified, cells were excluded from further analysis. In most cases displaying polysynaptic activity, however, the monosynaptic peak response was clearly identified as the leading peak with a latency that fell within 4 ms of EPSC onset. In a subset of cases (n = 4; 3 trained, 1 untrained) 1 μM TTX (Tocris Biosciences) and 100 μM 4-Aminopyridine (4-AP, Tocris Biosciences) was added to the bath to isolate monosynaptic input (Cruikshank et al., 2010; Petreanu et al., 2007; Petreanu et al., 2009) (Figure 1G). Importantly, the ratio of EPSC peak amplitudes between pairs of recorded cells remained the same when measuring the putative monosynaptic response under baseline conditions or in the presence of TTX and 4-AP.

The latency of EPSC onset varied across animals from 3-11 ms post-presentation of the photostimulus (mean 5.5 ± 3.3 ms). This variation was likely due to differential expression levels of ChR2 across animals, which affects the magnitude of light stimulation required for presynaptic release. Indeed, in slices with exceptionally low ChR2 expression (as assessed by eYFP expression level), light-evoked EPSCs were only observed with a photostimulus duration greater than 20 ms (such slices were excluded from analysis). Moreover, onset latency within animals showed minimal variability (mean SD for EPSC onset = 1± 0.9 ms). This minimal jitter further indicates that responses were monosynaptic.

For paired-pulse analysis, the peak response to each pulse was averaged over all trials, and the average response of the second response was divided by that to the first pulse. To preserve the relative differences in magnitude for ratios above and below a value of 1, the logarithm of each ratio was used for statistical comparisons. Cells displaying polysynaptic activity were excluded from the analysis.

Bulk photostimulation EPSC amplitude data were obtained from 77 cell pairs across 46 slices from a total of 32 animals. Because the number of cell pairs obtained per slice varied, we normalized the contribution of each slice to the overall data set by using the average response of all cell pairs for a given slice. Statistical analyses of the individual cell pair data did not affect statistical significance. These data were analyzed via Wilcoxon matched-pairs sign-rank test, the results of which are presented in text.

Progressive EPSC blockade via MK-801: To assess whether grasp training altered probability of release at TC terminals, NMDAR-mediated EPSCs were recorded in the presence of 20 µM (+)-MK-801 maleate (Tocris Biosciences) and 20 µM DNQX (Tocris Biosciences). In addition, 20 µM picrotoxin (Tocris Biosciences) was added to minimize interference from inhibitory currents. Neurons were held at +40 mV with a cesium-based internal solution consisting of 120 gluconic acid, 120 CsOH, 3 NaCl, 5 TEA-Cl, 10 HEPES, 9 EGTA, 2 ATP, 0.3 GTP, 3 phosphocreatine, and 3 QX-314. ChR2-expressing axons were stimulated with an inter-event interval of 25 s. At least 80 sweeps were recorded at +40mV, before and after which responses were assessed at -70mV to ensure AMPAR blockade was intact (see Figure 1D).

Strontium-evoked asynchronous release: To induce asynchronous vesical release at presynaptic TC terminals in response to ChR2 activation, calcium was replaced in the external solution with strontium (Gil et al., 1999; Kloc and Maffei, 2014; Petrus et al., 2014). The elimination of $Ca^{2+}$ depresses synchronous release of vesicles across presynaptic terminals following bulk stimulation, inducing prolonged, asynchronous release due to the ability of strontium to drive release and its slower removal from the presynaptic terminal relative to $Ca^{2+}$ (Xu-Friedman and

Regehr, 2000). In total, the external solution contained (in mM) 119 NaCl, 2.5 KCl, 1 NaHPO4, 2 MgSO4, 2 MgCl2, 26 NaHCO3, 20 glucose, and 3 SrCl2. Light was delivered via a 5x objective using a 470 nm LED (Thorlabs) for a duration of 100 - 300 ms (range of light intensities used = 0.5 – 3 $mW/mm^2$). Individual sweeps were separated by 25 s. Asynchronous release typically persisted for 500+ ms, as determined by an elevated mEPSC event frequency that was 5 - 18x greater than background. To identify individual TC release events, a template-based matching method was applied (Clements and Bekkers, 1997) to the region of elevated mEPSC event frequency (typically 60 – 500 ms post light stimulation, excluding the synchronous release component seen immediately following light stimulation (see Figure 4A)). A custom mEPSC template, 18 ms in duration, was created by averaging ~250 individual, manually selected events across multiple cells. This template was then used to identify individual mEPSC events by sliding it along individual current traces using pClamp 10 software. Fluctuations in postsynaptic current that sufficiently matched the duration and shape of the template (independent of amplitude) were counted as mEPSC events. A matching threshold of 2.8 was applied in order to minimize false positives without excessive loss of detection sensitivity in our recording conditions (see (Clements and Bekkers, 1997)). Further, the template method of identifying mEPSC events, in conjunction with our relatively high template matching threshold, inhibits overlapping, or "crashing", events from being collected (Clements and Bekkers, 1997). To further prevent crashing events from inclusion in our data set, events whose peak amplitude occurred > 5 ms beyond mEPSC onset were excluded from further analysis (this was rarely encountered).

All traces were low-pass filtered offline at 1 kHz prior to mEPSC detection. Cumulative distribution plots were generated using 100 randomly selected events for each neuron, and statistical significance was calculated using the Kolmogorov-Smirnov test.

AMPAR:NMDAR ratio: AMPAR-mediated responses were isolated by stimulating ChR2-expressing axons while holding the cell at -70mV. ChR2-expressing axons were stimulated with an inter-event interval of 25 s. At least 10 sweeps were recorded at this holding potential. NMDAR-mediated responses were subsequently isolated by bath application of the AMPAR antagonist DNQX (20 μM; Tocris Biosciences). In addition, 20 μM picrotoxin (Tocris Biosciences) was added to minimize interference from inhibitory currents. Neurons were held at +40 mV with the cesium-based internal solution referenced above. At least 40 sweeps were recorded at +40mV, before and after which responses were assessed at -70mV to ensure AMPAR blockade was intact. Peak responses were used to compute the AMPAR:NMDAR ratio.

Minimal optical stimulation: To examine the postsynaptic response due to stimulation of a single thalamocortical axon (McNaughton et al., 1981; Franks et al., 2011; Boyd et al., 2012), photostimulation intensity from a 470 nm LED (Thorlabs) was slowly increased from zero until a threshold postsynaptic response was detected on ~50% of

trials (that is, roughly half of light presentations resulted in synaptic failures). Once the appropriate stimulus intensity was found, 50 sweeps were recorded. Only recordings where the threshold intensity resulted in postsynaptic responses of consistent amplitude, suggesting the same thalamocortical axon was being stimulated across trials, were included for analysis.

Data analysis: Statistical comparisons were performed using JMP software, version 11.0 (SAS Institute). Unless otherwise noted, pairwise comparisons were made using Student's t-test or Wilcoxson's test for normal and non-normally distributed data, respectively. Normality was assessed by applying a fitted normal to each data set and assessing goodness-of-fit. Statistical tests were two-sided, and significance level was set at 0.05. In text, data values are presented as the mean ± standard deviation.

## SUPPLEMENTAL REFERENCES


Berndt, A., Schoenenberger, P., Mattis, J., Tye, K.M., Deisseroth, K., Hegemann, P., and Oertner, T.G. (2011). High-efficiency channelrhodopsins for fast neuronal stimulation at low light levels. Proc Natl Acad Sci U S A *108*, 7595-7600.

Biane, J.S., Scanziani, M., Tuszynski, M.H., and Conner, J.M. (2015). Motor cortex maturation is associated with reductions in recurrent connectivity among functional subpopulations and increases in intrinsic excitability. J Neurosci *35*, 4719-4728.

Boyd A.M., Sturgill J.F., Poo C., & Isaacson J.S. (2012). Cortical feedback control of olfactory bulb circuits. Neuron, 76(6):1161-74.

Clements, J.D., and Bekkers, J.M. (1997). Detection of spontaneous synaptic events with an optimally scaled template. Biophys J *73*, 220-229.

Conner, J.M., Culberson, A., Packowski, C., Chiba, A.A., and Tuszynski, M.H. (2003). Lesions of the Basal forebrain cholinergic system impair task acquisition and abolish cortical plasticity associated with motor skill learning. Neuron *38*, 819-829.

Clements J.D., Bekkers J.M. (1997). Detection of spontaneous synaptic events with an optimally scaled template. Biophys J 73(1):220-9.

Cruikshank, S.J., Urabe, H., Nurmikko, A.V., and Connors, B.W. (2010). Pathway-specific feedforward circuits between thalamus and neocortex revealed by selective optical stimulation of axons. Neuron *65*, 230-245.

Franks K.M., Russo M.J., Sosulski D.L., Mulligan A.A., Siegelbaum S.A., Axel R. (2011). Recurrent circuitry dynamically shapes the activation of piriform cortex. Neuron 72(1):49-56.

Gil, Z., Connors, B.W., and Amitai, Y. (1999). Efficacy of thalamocortical and intracortical synaptic connections: quanta, innervation, and reliability. Neuron *23*, 385-397.

Kloc, M., and Maffei, A. (2014). Target-specific properties of thalamocortical synapses onto layer 4 of mouse primary visual cortex. J Neurosci *34*, 15455-15465.

McNaughton BL, Barnes CA, & Andersen P (1981). Synaptic efficacy and EPSP summation in granule cells of rat fascia dentata studied in vitro. Journal of neurophysiology, 46(5):952-66

Petreanu, L., Huber, D., Sobczyk, A., and Svoboda, K. (2007). Channelrhodopsin-2-assisted circuit mapping of long-range callosal projections. Nat Neurosci *10*, 663-668.

Petreanu, L., Mao, T., Sternson, S.M., and Svoboda, K. (2009). The subcellular organization of neocortical excitatory connections. Nature *457*, 1142-1145.

Petrus, E., Isaiah, A., Jones, A.P., Li, D., Wang, H., Lee, H.K., and Kanold, P.O. (2014). Crossmodal induction of thalamocortical potentiation leads to enhanced information processing in the auditory cortex. Neuron *81*, 664-673.

Wang, L., Conner, J.M., Rickert, J., and Tuszynski, M.H. (2011). Structural plasticity within highly specific neuronal populations identifies a unique parcellation of motor learning in the adult brain. Proc Natl Acad Sci U S A *108*, 2545-2550.

Whishaw, I.Q. (2000). Loss of the innate cortical engram for action patterns used in skilled reaching and the development of behavioral compensation following motor cortex lesions in the rat. Neuropharmacology *39*, 788-805.

Xu-Friedman, M.A., and Regehr, W.G. (2000). Probing fundamental aspects of synaptic transmission with strontium. J Neurosci *20*, 4414-4422.